

# FEA OF VARIOUS DENTAL IMPLANT MATERIALS UNDER THE FATIGUE CRACK PROPAGATION MODEL USING ANSYS

Dr.A.Kalaiyaran, S.V.Srijan, G.Santhoshkumar, B.Sudhirkumar, M.Sandeepraj

<sup>1</sup>Assistant professor, Department of Mechanical Engineering, Muthayammal Engineering College, Rasipuram, Tamil Nadu, India  
-637408 Email ID: kalaianbutamil@gmail.com

<sup>2,3,4,5</sup>UG Student, Department of Mechanical Engineering, Muthayammal Engineering College, Rasipuram, Tamil Nadu, India -  
637408

## Abstract

The long-term stability of implants is greatly influenced by the selection of materials. Dental implants, which are subjected to cyclic loads during chewing, require materials with high resistance to fatigue. This study utilized finite element analysis to evaluate the performance of various materials (AISI 316L stainless steel, alumina, CoCr alloys, yttrium stabilized zirconia, zirconia-toughened alumina, and cp Ti with nanotubular TiO<sub>2</sub> surface) under real cyclic biting loads and determine the optimal material for implant applications. The mechanical behaviour and life of the implant were estimated based on material and surface properties. The results showed that the equivalent von Mises stress values ranged from 226.95 MPa to 239.05 MPa, and the penetration analysis revealed a range of 0.0037389mm to 0.013626 mm. The L-605 CoCr alloy-assigned implant model had the least penetration, while cp Ti with the nanotubular TiO<sub>2</sub> surface had the most. However, the difference was minimal. The fatigue life ranged from  $4 \times 10^5$  to  $1 \times 10^9$  cycles, indicating good performance for each evaluation component. Overall, considering mechanical performance and surface properties, cp Ti with the nanotubular TiO<sub>2</sub> surface material was deemed suitable for the designed dental implant model.

**Keywords:** Dental Implants, Finite Element Analysis, Material Selection, Equivalent von Mises stress, Penetration analysis, Fatigue analysis,

## 1. Introduction.

Biomaterials have a long history that can be traced back thousands of years, with evidence of metal dental implants being used in ancient civilizations. However, significant advancements in biomaterials occurred after World War II [1]. Biomaterials, in recent times, have been described as materials, either artificial or natural, that are utilized in the production of structures to replace damaged or diseased biological structures, thereby restoring their form and function. These biomaterials can interact with cells in a specific manner, resulting in predictable responses. The effectiveness of biomaterials is evaluated based on their bio functionality and biocompatibility [2]. The objective of this research is to evaluate and compare the performance of different biomaterials (Stainless Steel, Titanium, Alumina, CoCr alloy, Yttrium-stabilized zirconia, Zirconia-toughened alumina) in bone plate construction. The femur bone is modelled using SOLIDWORKS, and ANSYS is utilized for analysis. Additionally, fracture fixation plates are modelled, attached to a fractured bone, and thoroughly examined [3]. The durability of dental implants is a crucial concern, as they can experience failure over time due to cyclic life and fracture mechanisms. Accumulated damage over time is primarily attributed to the fracture mechanism, leading to catastrophic failure when deformation reaches a critical level [5]. The primary issue impacting the cyclic life is fatigue, which can be inferred. Fatigue behaviour and the lifespan of the implant material are determined by stress concentrations resulting from the threads' relative position within the implant structure and significant degradation of the material surface containing flaws [6]. The focus in this study was on selecting materials that would offer a satisfactory fatigue life. Fixation is a frequently observed problem in dental implants. The integration mechanism of the implant is based on the placement and then the quantity and quality of cortical and trabecular bones, which affect the primary stability and so the fixation of the implant [4]. In this context, the primary concern lies in the osseointegration process, where metallic implants are securely attached to the corresponding bone. The interaction between the implant and the bone is of utmost importance. However, the significant reduction in mandible dimensions caused by aging and the extensive atrophic changes lead to a loss of bone density, which becomes a critical factor in this interaction [2,7].

Implant placement is hindered due to the decrease in bone size and density [1]. To achieve optimization, various factors such as bone density, applied loads, implant dimensions, geometry and surface, bone-implant surface, and the quality and quantity of surrounding bone are considered and studied. Additionally, bone resorption is a significant complication that needs to be addressed in dental implant applications. By altering the surface properties of implants, it is possible to accelerate bone healing and promote bone growth. For instance, rougher surfaces can stimulate the differentiation, growth, and attachment of bone cells, as well as enhance mineralization [8]. The significance of roughness in this context cannot be overlooked, as specific implants are intentionally designed with rough surfaces during the manufacturing process [9].

Over the past few years, there has been a growing interest in exploring the surface characteristics of implants to enhance their ability to adhere to bone structures. Consequently, the focus of this study lies in examining and comparing porous materials

to achieve this goal. Another significant issue that arises is the lack of consistency between the implant and the surrounding bone tissue, which can lead to stress shielding, as highlighted in Elias et al.'s research [10].

The issue at hand is characterized by a significant difference in the elasticity of the bone and the implant, resulting in inadequate stress transfer to the bone due to the high modulus of the implant. To address this problem, it has been suggested that materials with a lower elastic modulus, closer to that of the bone tissues, can be used. These materials offer improved stress distribution at the implant-bone interface and can help reduce bone atrophy. Another technique mentioned in the literature involves utilizing porous materials and adjusting their porosity to match the elastic modulus of the human bone, which can also help eliminate the problem [11-13]. To address the issues, this study examined various implants based on their material composition. Our research group developed an implant model using different types of biomaterials, including AISI 316L stainless steel, alumina (both porous and non-porous), CoCr alloys, yttrium-stabilized zirconia (YSZ), zirconia-toughened alumina (ZTA), and cp Ti with a nanotubular TiO<sub>2</sub> surface. Through simulations with real cyclic biting loads, we investigated the stress distribution on the implant, the interaction between the implant and bone, and the longevity and stability of the implants. Additionally, we discussed the impact of different materials on implant performance and determined the optimal material properties for dental implants in fatigue conditions.

## 2. Materials and Methods

### 2.1 CAD Model Preparation of the Implant and Abutment.

To create an FEA model, a reference implant-abutment model was required. To meet the criteria, a design of the implant was generated using SolidWorks 2012 from Dassault Systems in France. This implant model has a nonthreaded cylindrical neck with a height of 2.0 mm and a threaded part with a height of 11.0 mm. It has a diameter of 4.5 mm and a length of 13.0 mm. The thread detail was based on an implant model (Advent) from Zimmer Dental, Inc., a trademark from CA, USA. In Figure 1, technical drawing of the implant-abutment system is shown.

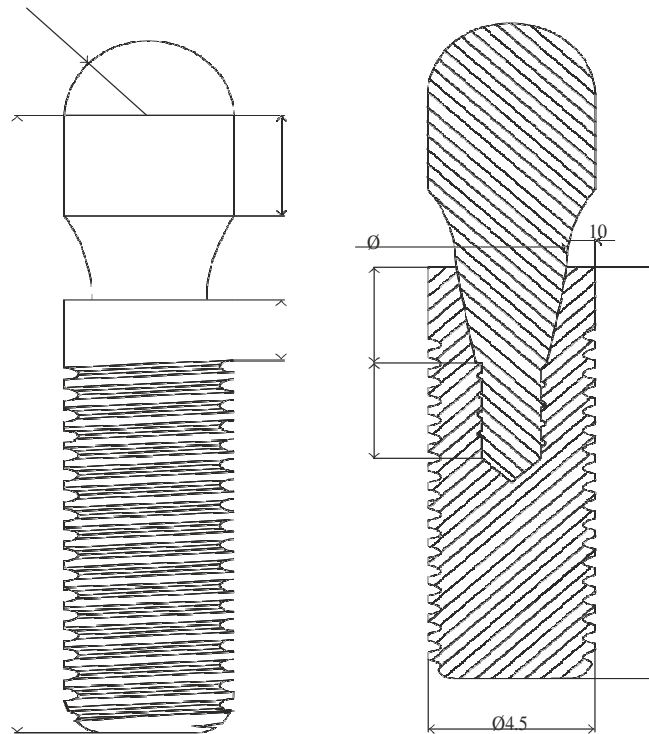


Figure 1 Side and sectional views and main dimensions of the implant and abutment assembly.

### 2.2 FEA Model Preparation of the Implant and Abutment.

The CAD data was prepared for Finite Element Analysis (FEA) to evaluate the impact of various dental implant materials. The ISO 14801 standards were followed to set the conditions. Using CAD software, the implant, abutment, and implant holder

were assembled and then exported to ANSYS Workbench 2023 R2 software by ANSYS, Inc. in the USA. The method of "tetrahedrons" was employed to establish the mesh configuration, resulting in the generation of 10-node tetrahedral elements. To achieve finer meshes, the body sizing option was utilized for all bodies, incorporating the "sphere of influence" option. The critical region, located near the second thread from the head of the implant, served as the centre of the sphere, with an element size of 0.6 mm. In accordance with Ferreira et al.'s study, frictional contacts were defined to establish the frictional connection, with a coefficient of 0.3 [15].

The contact solution formulation for the assembled structure bodies involved the use of the "Augmented Lagrange" option, while the interface treatment included the "Adjust to Touch" option. The boundary condition was set with the lateral surface nodes of the implant holder being fixed supported. According to the literature, a 100 N load falls within the normal bite force range. Hence, in this study, a 100 N load was applied to the top surface of the abutment at a 30° inclination, following the ISO 14801 standard [16,17]. To simulate real conditions as accurately as possible, the abutment was tightened with a torque of 30 N cm, as per the implant manufacturer's recommendation [14]. Figure 2 shows the brief FEA conditions.

### 2.3 Material Selection and Assignment to the Bodies of the Model.

To obtain a finite element solution for the model, it was necessary to accurately assign material properties to all bodies in the model. Extensive research was conducted on both conventional and novel biomaterials, following the criteria mentioned in the study's introduction, to determine their suitability for dental applications. Ti alloys, AISI 316L stainless steel, CoCr alloys, alumina, zirconia-toughened alumina (ZTA), and yttrium-stabilized zirconia (YSZ) have been identified as potential alternative materials for dental implants and continue to be studied [18-21]. Figure 1 Side and sectional views and main dimensions of the implant and abutment assembly. It is advisable to provide a detailed explanation and conduct comprehensive comparisons of the materials being considered to support the reasons behind their selection. Upon reviewing the literature, it becomes evident that AISI 316L stainless steel is the preferred choice for dental implant applications due to its affordability, resistance to corrosion, and ease of production [18].

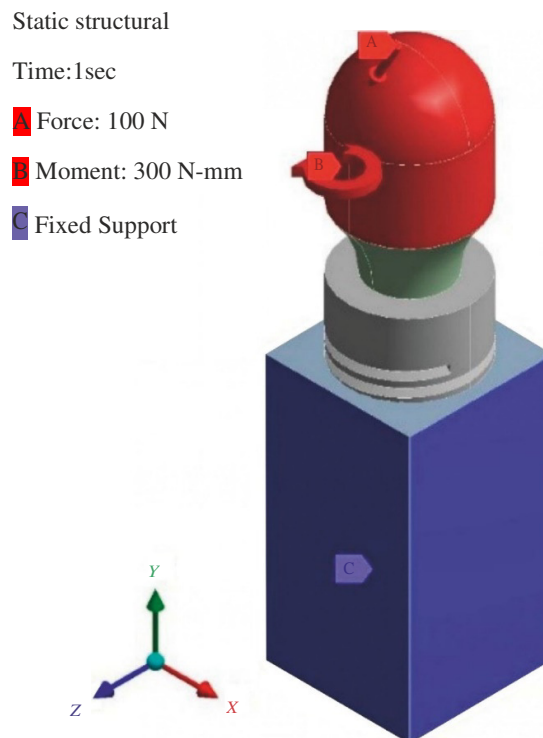


Figure 2 Isometric view of the FEA initial conditions.

Furthermore, an extra layer of coating is favoured to reduce the build-up of ions in the affected area of the bone because of the alloy's compound elements. CoCr is another type of alloy that can be utilized in dental implant applications. It is highly regarded for its exceptional corrosion resistance, thanks to the presence of chrome-based oxides on its surface, which creates a protective layer. As a result, the implant surface remains smoother even when exposed to saliva, indicating a lower degradation process compared to other commercial alloys like titanium [19]. Manufacturing this material can be challenging and time-consuming, which limits its usage. However, ceramic materials are experiencing a rise in usage. Ceramic implants are gaining popularity among patients and clinicians because of their excellent wear resistance and relatively superior biocompatibility.

Porous alumina, a popular ceramic material structure, is known for its biocompatibility in porous form and allows tissue ingrowth, which is crucial for implant stabilization [21]. In this study, the potential use of porous alumina as dental implants was explored, along with the investigation of yttria-stabilized tetragonal zirconia (YSZ). YSZ is considered a preferred material for dental implants due to its excellent flexural strength (ranging from 800 to 1000 MPa), toughness, corrosion resistance, and wear resistance [22,23].

Table 1 The properties of materials used in this study.

| Materialname                                      | Density (g/cm <sup>3</sup> ) | Young's Modulus (Gpa) | Poisson's Ratio | Ultimate Tensile Strength (Mpa) | Reference Number |
|---|------------------------------|-----------------------|-----------------|---------------------------------|------------------|
| AISI316Lstainlesssteel                            | 8.00                         | 192                   | 0.30            | 860                             | [27–29]          |
| Nanoporousanodicalumina                           | 3.96                         | 370                   | 0.22            | 220                             | [30,31]          |
| L-605CoCralloy                                    | 9.24                         | 240                   | 0.29            | 1180                            | [32]             |
| cp Tiwith thenanotubular TiO <sub>2</sub> surface | 3.89                         | 40                    | 0.31            | 640                             | [33,34]          |
| Yttrium-stabilizedzirconia(YSZ)                   | 6.05                         | 197                   | 0.33            | 432                             | [35–37]          |
| Zirconia-toughenedalumina(ZTA)                    | 4.10                         | 310                   | 0.26            | 760(flexural)                   | [38]             |
| Trabecularbone                                    | —                            | 1.38                  | 0.30            | —                               | [39]             |

In addition, zirconia can enhance the strength and toughness of alumina. When tetragonal-phase zirconia is added to alumina, it increases the material's strength and fracture toughness while only slightly reducing its hardness and elastic modulus [24,25]. Kurtz et al. suggest that by increasing fracture toughness, it becomes possible to produce thinner liners, which in turn reduces the chances of impingement and dislocation, while enhancing the stability of the implants [25]. Upon examining the literature, it is evident that titanium (Ti) is commonly found as a base material in both metallic alloy and ceramic forms. Metallic alloy variations of Ti have been utilized in dental implants due to their exceptional strength and fatigue resistance. Nevertheless, these alloys may pose a potential toxicity risk due to the presence of vanadium and aluminium. As a result, commercially pure grades of Ti are favoured to mitigate any potential adverse effects [26]. In addition, the implants need to have a certain level of roughness to improve their connection with trabecular bone tissue. This requirement can be fulfilled either during the manufacturing process or by using specific material properties. To explore this further, the mechanical properties of novel materials such as nanoporous anodic alumina and nanotubular titanium oxide were compared with other materials. These materials were included in the FEA solver along with their respective mechanical properties listed in Table 1. Furthermore, the fixture was set as the trabecular bone to observe its response under loading conditions.

**2.4 Fatigue Analysis Procedure.**

In addition to static analysis, a successful dental implant should also demonstrate sufficient durability over time [6]. The fatigue analysis of the implant model was conducted using the fatigue tool of ANSYS Workbench 16.2, which utilizes fatigue FEA to determine the cyclic performance of materials and designs. The solver was provided with the S-N curves data of the relevant materials to perform the analysis. [37, 40-43]. The cyclic properties of the porous and tubular structures have exemption data in this process. These properties are typically assessed based on the main or base material, and for the nanotubular and nanoporous structures, S-N data were chosen using bulk cp Ti and alumina materials. Furthermore, the fatigue life analysis was conducted using the Goodman fatigue theory, which considers the tensile strength values of the materials, particularly for brittle materials [44].

**3. Result and Discussion**

The static FEA analysis yielded results for both the equivalent stress and the penetration into the bone structure, which were subsequently examined. Subsequently, the fatigue life calculations were performed using the equivalent stress data, and their findings were also discussed.

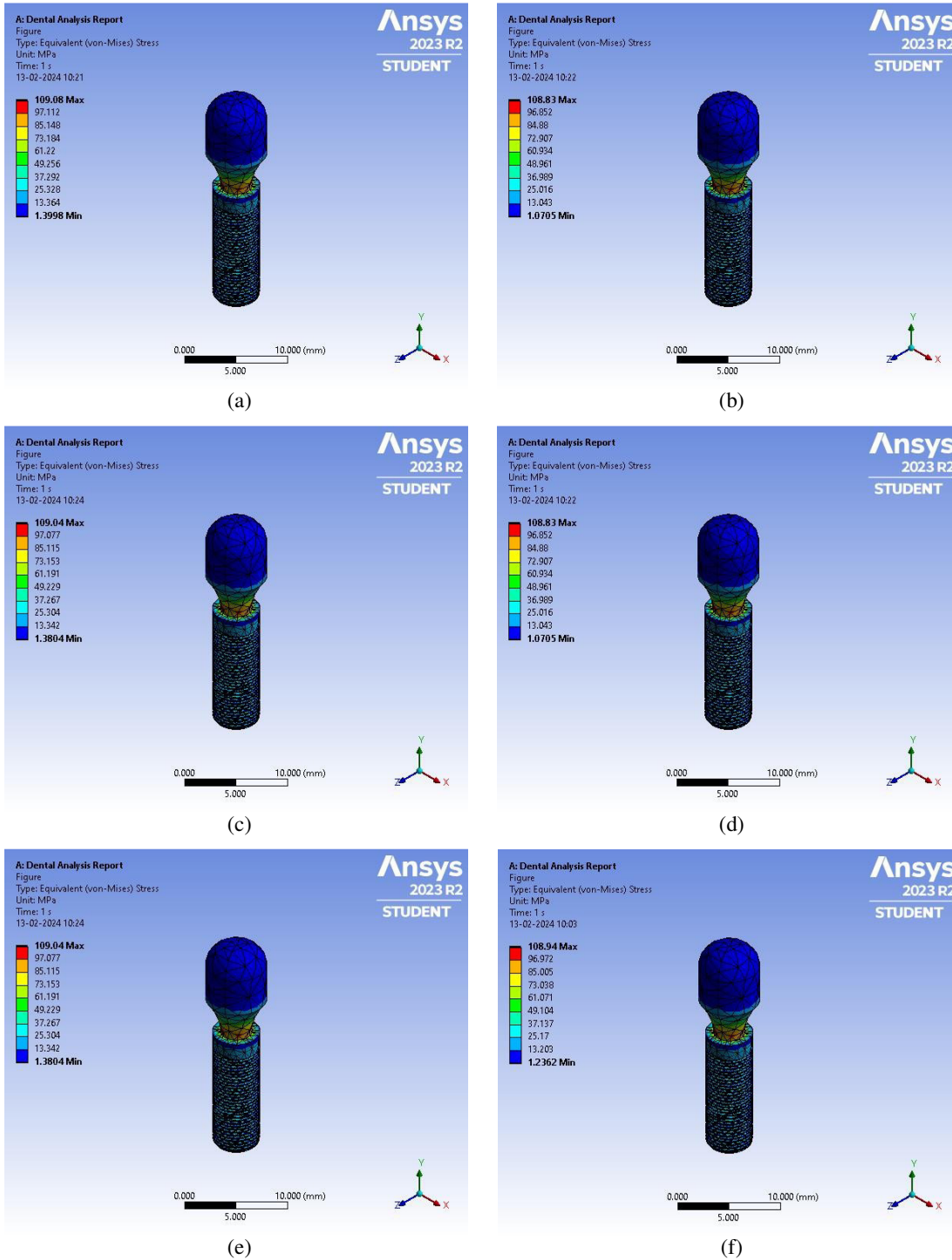


Figure 3: FEA results of implants. Implant materials are AISI 316L stainless steel (a), nanoporous anodic alumina (b), L-605 CoCr alloy (c), cp Ti with the nanotubular TiO<sub>2</sub> surface (d), YSZ (e), and ZTA (f).

### 3.1 Equivalent (von Mises) Stress Values.

Figure 3 displays the concentrated regions and corresponding von Mises stress values. The first thread in all models exhibited the highest von Mises stresses, indicating that the critical region can be identified as the initial knuckle. This finding aligns with the research conducted by Wang et al [45]. Hence, it is possible that these implants may fracture or fail in the thread region due to design-related issues. However, the design is not the focus of this study as all the models have the same design. The

calculated equivalent stress values range from 226.95 MPa to 239.05 MPa, which are relatively close to each other. The equivalent stress depends on the implant dimensions, loading conditions, elastic modulus, and Poisson's ratio of the materials. In terms of FEM theory, the results are typically evaluated based on elastic behaviour for static analysis, and the stress values are determined using basic strength calculations and theories.

These values are also influenced by the amount of deformation, which is compensated by the couple terms. Therefore, the results should be discussed in this context, and the slight differences in stress values can be attributed to this compensation, indicating varying deformation in the models. Furthermore, considering the Poisson's ratio values, the model with YSZ material tends to exhibit more transversal deformation compared to the others due to its higher Poisson's ratio. As a result, the first knuckle of this material's model may experience the most deformation, leading to the highest equivalent stress value.

### **3.2 Penetration onto the Bone.**

The primary limitations for this study are the stress state, cyclic life, and the compatibility of implant materials with the bone, apart from deformation. To ensure optimal stress transfer and prevent the stress-shielding effect, it is crucial for the implant's elastic modulus to closely match that of the bone [46].

The materials of cp Ti with the nanotubular TiO<sub>2</sub> surface, YSZ, and AISI 316L stainless steel are highly regarded due to their relatively low elastic modulus. The nanotubular titania structure exhibits the lowest elastic modulus value, which is closest to that of bone. This material induces the highest von Mises stress on the implant model, as its low elastic modulus allows for more deformation on the structure. Consequently, stress shielding is prevented, and smooth stress transfer is achieved instead of severe stress transfer to the bone. The proximity of Young's modulus becomes crucial at this stage, and various methods exist to calculate it for cp Ti with the nanotubular TiO<sub>2</sub> surface. One such method involves using an equation based on the Berkovich indentation technique, which considers contact stiffness, maximum load, and depth [47].

The second method is simpler but still valuable as it provides a close approximation. It utilizes the rule of mixtures technique commonly used for continuous fibre-reinforced composites. This method assumes the structure is either in the isostrain or isostress condition, with the orientation determining the Young's modulus of the composite. Consequently, the Young's modulus of the cp Ti with the nanotubular TiO<sub>2</sub> surface can vary depending on the fraction of nanotubes and their direction. By adjusting the tubular structure, the Young's modulus can be modified. This suggests that nanotubular titania tends to absorb stress and deform to a greater extent.

To further investigate, it is appropriate to study the penetration amounts of the implant models into the bone, as depicted in Figure 4. The implant model with cp Ti and nanotubular TiO<sub>2</sub> surface had the highest penetration onto the bone structure, measuring 0.013626 mm. On the other hand, the implant model with L-605 CoCr alloy had the lowest penetration, measuring 0.0037389 mm. Although the highest result indicates a significant penetration value at the microscale, the difference between these extreme penetration amounts is approximately 0.01 mm.

Therefore, evaluating the penetration amount alone is not sufficient. The surface roughness and bone adsorption also play a crucial role. Coelho et al. suggest that different methods of implant surface engineering can result in unique surface properties, which can impact the host-to-implant response. They emphasize the need to test and evaluate new implant surfaces as new biomaterials [9]. The use of materials with nanotubular and nanoporous structures may be beneficial for manufacturing implants due to their ability to accelerate bone healing and growth. However, when considering their unique mechanical properties, it is important to note that the model with nanoporous anodic alumina exhibits a von Mises stress magnitude of 237.56 MPa, which exceeds its ultimate tensile strength value. This suggests that the nanoporous region may become damaged, indicating the need for further study and development of this material. As a result, nanotubular titania emerges as a prominent alternative.

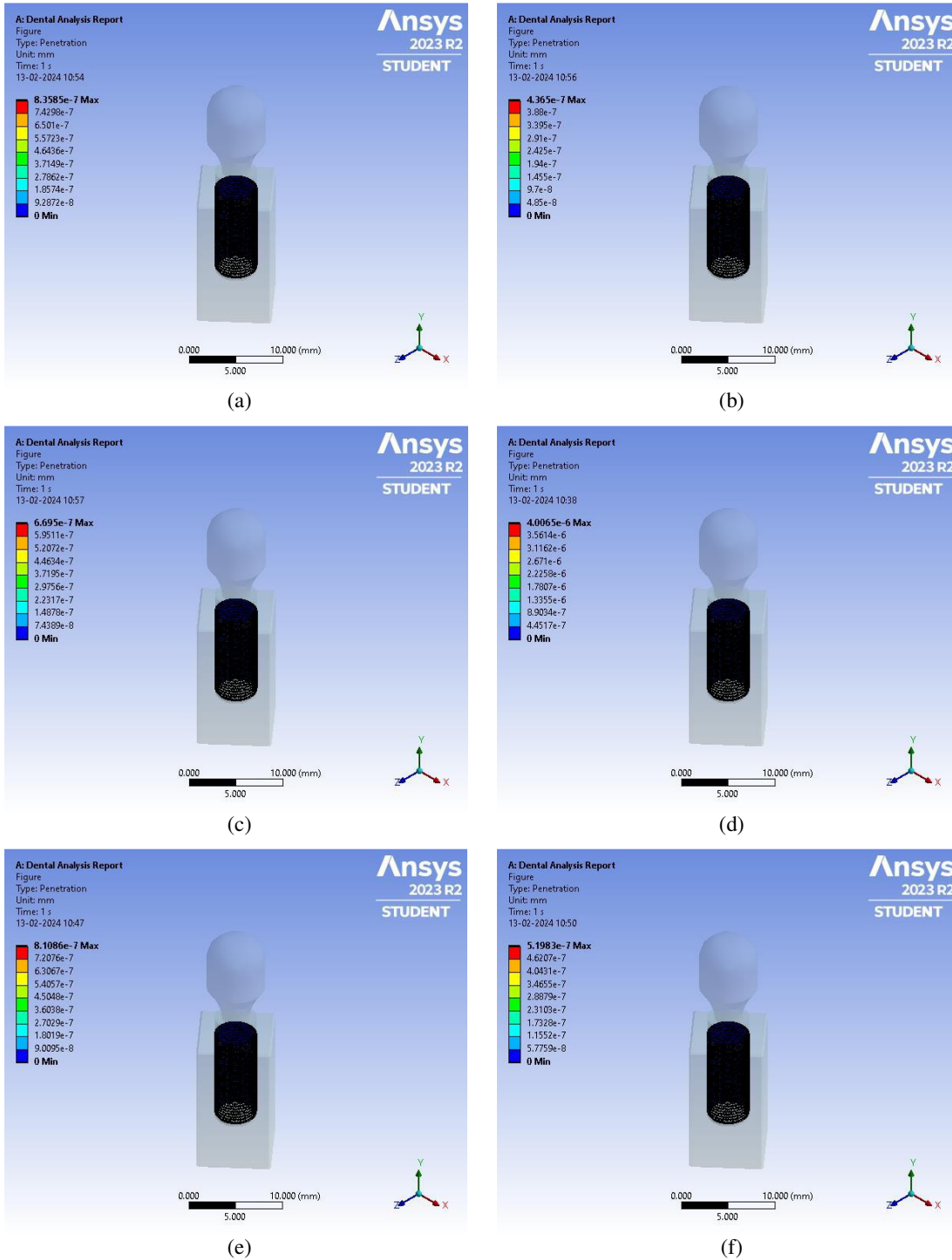


Figure 4: Bone penetration results of implants. Implant materials are AISI 316L stainless steel (a), nanoporous anodic alumina (b), L-605 CoCr alloy (c), cp Ti with the nanotubular TiO2 surface (d), YSZ (e), and ZTA (f).

### 3.3 Fatigue Life Results.

The prediction of life is determined by the cycle number that corresponds to the cyclic stress value. Yona et al. also suggest that materials are being sought to ensure an "infinite" lifespan in the S-N curve for dental implants under the relevant loading condition, to address the issue at hand [6]. Figure 5 displays the results of fatigue life prediction. The S-N curve data obtained from literature is utilized with a loading ratio of  $R = -1$  for running the solver. The cycle results fall within the range of  $(4 \times 10^5)$  and  $(1 \times 10^9)$ . To evaluate the outcomes, the recommended value of  $(5 \times 10^6)$  cycles, as stated in the guideline of the Dental Device Branch of FDA (U.S. Department of Health and Human Services-Food and Drug Administration), is employed [49]. The mentioned text can serve as a point of reference for fulfilling the life cycle requirement of implants.

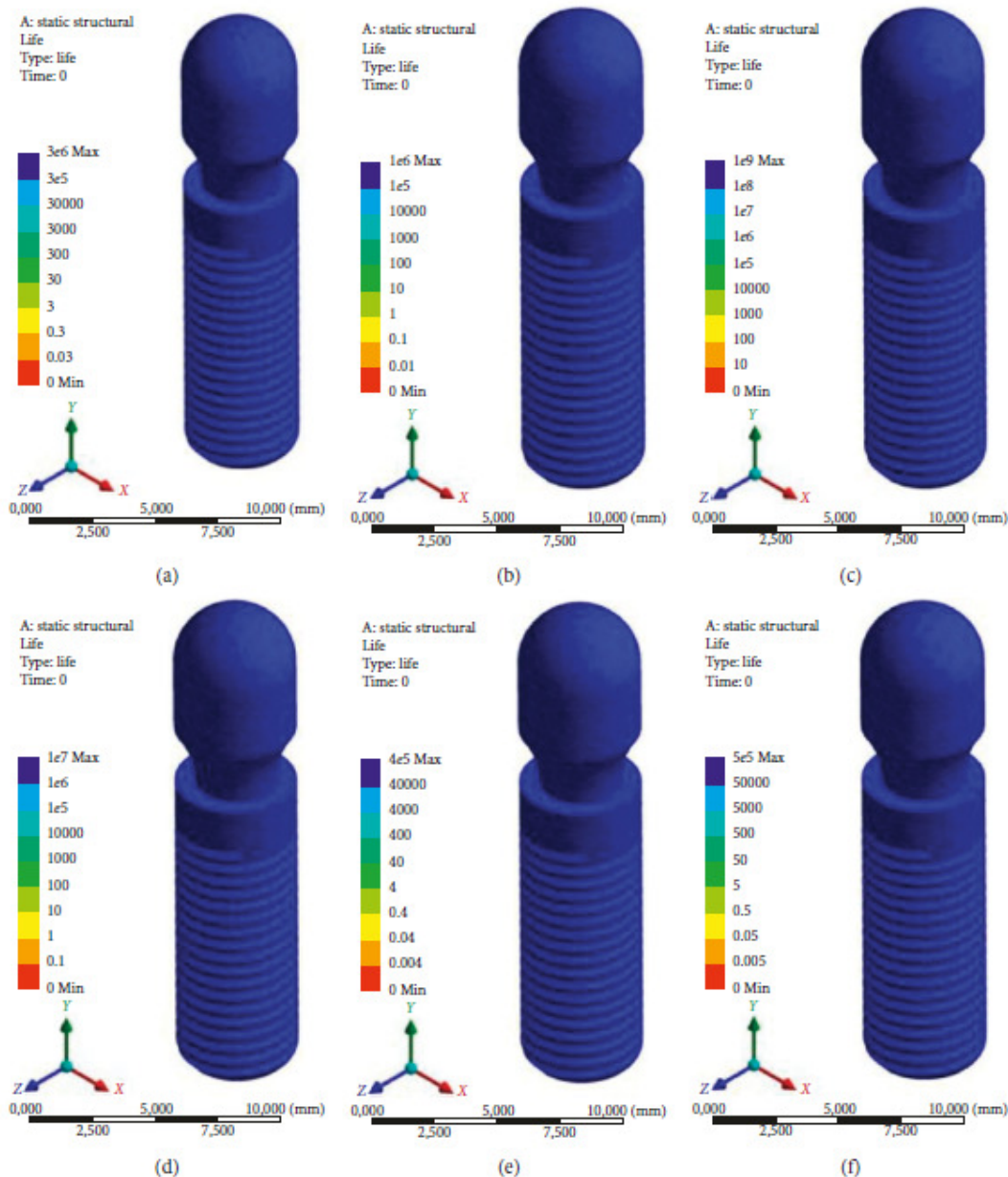


Figure 5: Fatigue life results of implants. Implant materials are AISI 316L stainless steel (a), nanoporous anodic alumina (b), L-605 CoCr alloy (c), cp Ti with the nanotubular TiO<sub>2</sub> surface (d), YSZ (e), and ZTA (f).

The implant, which was modelled using cp Ti with a nano-tubular TiO<sub>2</sub> surface, demonstrated a lifespan of  $(1 \times 10^7)$  cycles, while the CoCr alloy-assigned model exhibited a lifespan of  $(1 \times 10^9)$  cycles. Therefore, these models not only meet but



also surpass the specified life expectancy. However, other materials appear to fall short in meeting the life criteria for the respective implant model.

However, titanium alloy implants have been associated with treatment failure due to high cyclic loading, leading to resorption of the peri-implant bone and increased bending moments on the implants, ultimately resulting in fracture [36]. In contrast, the use of nanotubular TiO<sub>2</sub> surface structure on commercially pure titanium (cp Ti) implants is predicted to decrease bone resorption. Furthermore, it is likely to enhance bone growth and adsorption, offering a potential solution to the problem. In summary, based on the finite element analysis (FEA) results, the utilization of cp Ti with nanotubular TiO<sub>2</sub> surface appears to be a reasonable approach.

### 3.4 Thread Number Effect on the Fixation of the Implant.

The study found that cp Ti with the nanotubular TiO<sub>2</sub> surface performed the best overall. An additional analysis was conducted to examine the impact of thread numbers on the implant structure. Increasing the roughness surface can help improve fixation and prevent loosening of the implant screw. Two- and three-threaded designs with the same total pitch were developed and analysed to assess stress levels and distribution. The results, along with the mechanical properties of cp Ti with the nanotubular TiO<sub>2</sub> surface, are presented in Figure 6. The von Mises stress values exhibit similarity and reasonability, although the one-threaded design yields a higher result of 239.05 MPa compared to the multithreaded designs. This discrepancy can be attributed to the distribution of stress over a larger surface area in the multithreaded designs, resulting in lower stress values. However, the presence of more grooves in the multithreads introduces a potential notch effect, leading to unpredictable failure or damage. Therefore, it is necessary to conduct in vitro tests to validate the effectiveness of the multithreaded design approach. To optimize the design, it is advisable to avoid sharp threads and minimize the thread angles at the junction region of the implant body. Additionally, the depth of the thread should be adjusted to prevent interference with the bone, thereby increasing friction and preventing implant failure due to screw loosening. Furthermore, instead of utilizing porous or nanotubular structures, the roughness can be enhanced by incorporating multiple threaded designs or altering the thread section to achieve mechanical locking between the implant surface and the surrounding bone tissue.

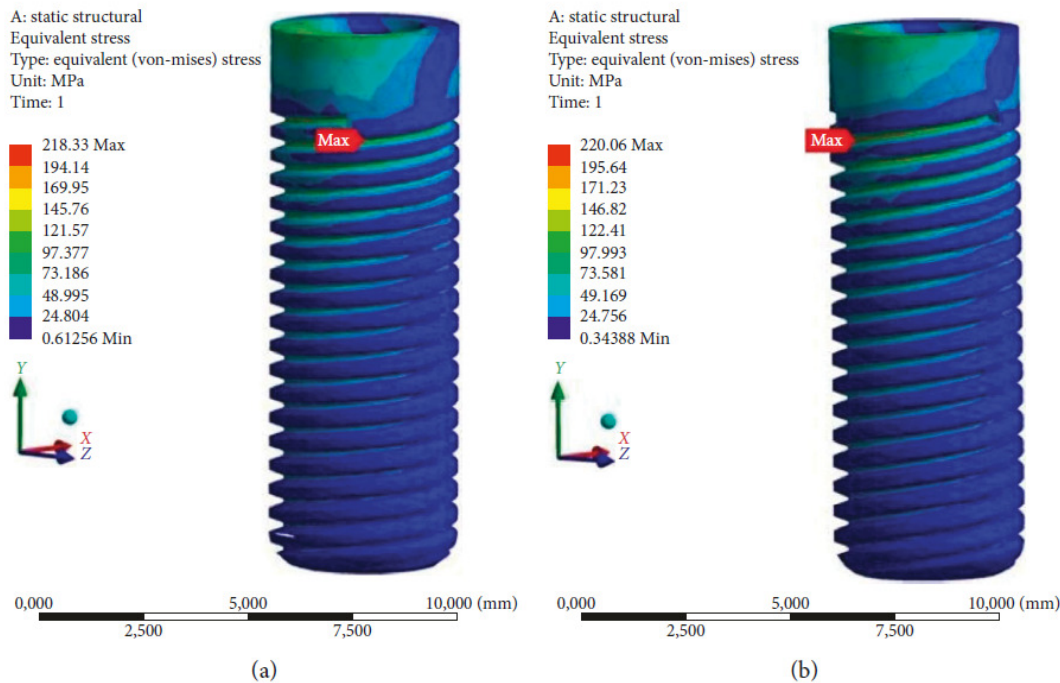


Figure 6: FEA results of implants with 2 threads (a) and 3 threads (b). The implant material is cp Ti with the nanotubular TiO<sub>2</sub> surface.

#### 4. Conclusion

The discussion focused on the impact of biomaterials on the stress and fatigue of dental implants, as well as their interaction with bone. Several biomaterials suitable for implant use were examined, and the study yielded the following findings when subjected to cyclic biting loads.

- i. Stress distribution on the implant is influenced by the mechanical properties of the implant materials. The stress magnitude and distribution are particularly affected by the elastic modulus. Additionally, Poisson's ratio is another factor that is closely related to the elastic modulus and influences the deformation and stress simultaneously.
- ii. When the elastic modulus of an implant matches that of the bone, any applied load results in stress and increased deformation on the implant. This allows for a seamless transfer of stress from the implant to the bone, reducing the magnitude of transmitted energy. Consequently, the interaction between the implant and the bone becomes smoother. Although this leads to more deformation in both the implant and bone tissue, it can also be seen as less damaging to the bone since the implant is not excessively rigid, resulting in less bone pulverization.
- iii. The increase in implant deformation results in a decrease in elasticity, which in turn leads to an increase in implant to bone penetration. Therefore, it is advisable to conduct further research on the medical interaction involved in this phenomenon.
- iv. To enhance stability, it is necessary to increase the friction. Therefore, utilizing multiple threaded designs can be considered as a potential solution to achieve the necessary mechanical bonding between the implant surface and the adjacent bone.
- v. The TiO<sub>2</sub> dental implant with nanoporous/nanotubular structure and multiple threaded designs is suitable for implantation technology. It has a similar elastic modulus to bone tissue, allowing for smooth stress transfer from the implant to the bone. The nanoporous surface and multiple threaded design enhance surface roughness and friction, promoting better implant fixation and supporting bone growth. Additionally, this implant's novel design and high strength contribute to its long-term stability even under cyclic biting loads.

#### Conflicts of Interest

The authors affirm that there are no competing interests associated with the publication of this paper.

#### References

- [1] A Kalaiyarasan, K Sankar, S Sundaram - *Finite element analysis and modelling of fractured femur bone - Materials Today: Proceedings*, 2020.
- [2] K Sankar A Kalaiyarasan, D Sasikala, S Selvarasu - *Finite Element Analysis of Fractured Femur Bone with Prosthetic Bone Plates Using ANSYS Software - Cardiometry*, 2023.
- [3] A Kalaiyarasan, K Sankar, M Madheswaran, C Harish - *Finite Element Analysis of Femur Bone under Different Loading Conditions - 2021 International Conference on Computational2021*.
- [4] P.Bicudo, J.Reis, A.M. Deus, L. Reis, and M.F. Vaz, "Mechanical behaviour of dental implants," *Procedia Structural Integrity*, vol. 1, pp. 26-33, 2016.
- [5] S. Suresh, "Stress-life approach," in *Fatigue of Materials*, Cambridge University Press, Cambridge, UK, 2nd edition, 1998.
- [6] K. S. Yona and D. Rittel, "Fatigue of dental implants: facts and fallacies," *Dentistry Journal*, vol. 4, no. 2, p. 16, 2016.
- [7] F. Lofaj, J. Kucera, D. Nemeth, and L. Kvetkova, "Finite element analysis of stress distributions in mono- and bi-cortical dental implants," *Materials Science and Engineering C*, vol. 50, pp. 85-96, 2015.
- [8] A. B. Novaes Jr., S. L. S. Souza, R. R. M. Barros, K. K. Y. Pereira, G. Iezzi, and A. Piattelli, "Influence of implant surfaces on osseointegration," *Brazilian Dental Journal*, vol. 21, no. 6, pp. 471-481, 2010.
- [9] P. G. Coelho, J. M. Granjeiro, G. E. Romanos et al., "Basic research methods and current trends of dental implant surfaces," *Journal of Biomedical Materials Research Part B: Applied Biomaterials*, vol. 88, no. 2, pp. 579-596, 2009.
- [10] C. N. Elias, D. J. Fernandes, C. R. S. Resende, and J. Roestel, "Mechanical properties, surface morphology and stability of a modified commercially pure high strength titanium alloy for dental implants," *Dental Materials*, vol. 31, no. 2, pp. 1-13, 2015.
- [11] J. Chen, C. Rungsiyakull, W. Li, Y. Chen, M. Swain, and Q. Li, "Multiscale design of surface morphological gradient for osseointegration," *Journal of the Mechanical Behavior of Biomedical Materials*, vol. 20, pp. 387-397, 2013.
- [12] E. D. Spoerke, N. G. Murray, H. Li, L. C. Brinson, D. C. Dunand, and S. I. Stupp, "A bioactive titanium foam scaffold for bone repair," *Acta Biomaterialia*, vol. 1, no. 5, pp. 523-533, 2005.
- [13] C. M. Abraham, "A brief historical perspective on dental implants, their surface coatings and treatments," *Open*

- Dentistry Journal, vol. 8, no. 1, pp. 50–55, 2014.
- [14] Zimmer Biomet, Dental, [http://www.zimmerdental.com/library/lib\\_techtipsfaq.aspx](http://www.zimmerdental.com/library/lib_techtipsfaq.aspx), 2017.
- [15] M. B. Ferreira, V. A. Barao, J. A. Delben, L. P. Faverani, A. C. Hipolito, and W. G. Assuncao, “Non-linear 3D finite element analysis of full-arch implant-supported fixed dentures,” *Materials Science and Engineering C*, vol. 38, pp. 306–314, 2014.
- [16] B. C. Spies, C. Sauter, M. Wolkewitz, and R. J. Kohal, “Alumina reinforced zirconia implants: effects of cyclic loading and abutment modification on fracture resistance,” *Dental Materials*, vol. 31, no. 3, pp. 262–272, 2015.
- [17] M. A. L. H. Rodriguez, G. R. C. Hernandez, A. J. Hernandez, B. B. Ramirez, and E. G. Sanchez, “Failure analysis in a dental implant,” *Engineering Failure Analysis*, vol. 57, pp. 236–242, 2015.
- [18] M. H. Fathi, M. Salehi, A. Saatchi, V. Mortazavi, and S. B. Moosavi, “In vitro corrosion behaviour of bioceramic, metallic, and bioceramic-metallic coated stainless steel dental implants,” *Dental Materials*, vol. 19, no. 3, pp. 188–198, 2003.
- [19] L. Hjalmarsson, *On Cobalt-Chrome Frameworks in Implant Dentistry*, Geson Hylte Tryck, Gothenborg, Sweden, 2009.
- [20] G. Maccauro, P. R. Iommetti, L. Raiaelli, and P. F. Manicone, “Alumina and zirconia ceramic for orthopaedic and dental devices,” in *Biomaterials applications for Nanomedicine*, R. Pignatello, Ed., InTech, Rijeka, Croatia, 2011.
- [21] J. J. Klawitter, A. M. Weinstein, F. W. Cooke, L. J. Peterson, B. M. Pennel, and R. V. McKinney Jr., “An evaluation of porous alumina ceramic dental implants,” *Journal of Dental Research*, vol. 56, no. 7, pp. 768–776, 1977.
- [22] R. B. Osman and M. V. Swain, “A critical review of dental implant materials with an emphasis on titanium versus zirconia,” *Materials*, vol. 8, no. 3, pp. 932–958, 2015.
- [23] G. S. Kaliaraj, M. Bavanilathamuthiah, K. Kirubakaran et al., “Bioinspired YSZ coated titanium by EB PVD for biomedical applications,” *Surface and Coatings Technology*, vol. 307, pp. 227–253, 2016.
- [24] X. He, Y. Z. Zhang, J. P. Mansell, and B. Su, “Zirconia toughened alumina ceramic foams for potential bone graft applications: fabrication, bioactivation, and cellular responses,” *Journal of Materials Science: Materials in Medicine*, vol. 19, no. 7, pp. 2743–2749, 2008.
- [25] S. M. Kurtz, S. Kocagoz, C. Arnholt, R. Huet, M. Ueno, and W. L. Walter, “Advances in zirconia toughened alumina biomaterials for total joint replacement,” *Journal of the Mechanical Behavior of Biomedical Materials*, vol. 31, pp. 107–116, 2014.
- [26] C. N. Elias, J. H. C. Lima, R. Valiev, and M. A. Meyers, “Biomedical applications of titanium and its alloys,” *JOM*, vol. 60, no. 3, pp. 46–49, 2008.
- [27] B. Gervais, A. Vadean, M. Raison, and M. Brochu, “Failure analysis of a 316L stainless steel femoral orthopaedic implant,” *Case Studies in Engineering Failure Analysis*, vol. 5-6, pp. 30–38, 2016.
- [28] L. H. Timmins, C. A. Meyer, M. R. Moreno, and J. E. Moore, “Effects of stent design and atherosclerotic plaque composition on arterial wall biomechanics,” *Journal of Endovascular Therapy*, vol. 15, no. 6, pp. 643–654, 2008.
- [29] M. McCracken, “Dental implant materials: commercially pure titanium and titanium alloys,” *Journal of Prosthodontics*, vol. 8, no. 1, pp. 40–43, 1999.
- [30] T. H. Fang, T. H. Wang, C. H. Liu, L. W. Ji, and S. H. Kang, “Physical behaviour of nanoporous anodic alumina using nanoindentation and microhardness tests,” *Nanoscale Research Letters*, vol. 2, no. 8, pp. 410–415, 2007.
- [31] K. Davis, “Material review: alumina (Al<sub>2</sub>O<sub>3</sub>),” *School of Doctoral Studies (European Union) Journal*, vol. 2, pp. 109–114, 2010.
- [32] ASM Materials for Medical Devices Database Committee, *Materials and Coatings for Medical Devices: Cardiovascular*, ASM International, Geauga County, OH, USA, 2009.
- [33] S. Sobieszczyk and R. Klotzke, “Nanotubular titanium oxide layers for enhancement of bone-implant bonding and bioactivity,” *Advances in Materials Sciences*, vol. 11, no. 1, pp. 17–26, 2011.
- [34] T. Yoshimura, H. Imai, T. Threrujirapapong, and K. Kondoh, “Cost effective pure titanium with high mechanical response by oxide dispersion strengthening,” *Materials Transactions*, vol. 50, no. 12, pp. 2751–2756, 2009.
- [35] M. Oishi, Y. Matsuda, K. Noguchi, and T. Masaki, “Evaluation of tensile strength and fracture toughness of yttria-stabilized zirconia polycrystals with fracture surface analysis,” *Journal of the American Ceramic Society*, vol. 78, no. 5, pp. 1212–1216, 1995.
- [36] K. Noguchi, Y. Matsuda, M. Oishi, T. Masaki, S. Nakayama, and M. Mizushima, “Strength analysis of yttria-stabilized tetragonal zirconia polycrystals,” *Journal of the American Ceramic Society*, vol. 73, no. 9, pp. 2667–2676, 1990.
- [37] S. Y. Liu and I. W. Chen, “Fatigue of yttria-stabilized zirconia: I, fatigue damage, fracture origins, and lifetime prediction,” *Journal of the American Ceramic Society*, vol. 74, no. 6, pp. 1197–1205, 1991.
- [38] K. J. Anusavice, C. Shen, and H. R. Rawls, *Phillips’ Science of Dental Materials*, Elsevier, Amsterdam, Netherlands, 12th edition, 2012.
- [39] M. Sevimay, A. Usumez, and G. Eskitascioglu, “The influence of various occlusal materials on stresses transferred to implant-supported prostheses and supporting bone: a three-dimensional finite-element study,” *Journal of Biomedical Materials Research Part B: Applied Biomaterials*, vol. 73, no. 1, pp. 140–147, 2005.
- [40] H. E. Boyer, *Atlas of Fatigue Curves*, ASM International, Geauga County, OH, USA, 1986.
- [41] R. Nejma, K.-H. Lang, and D. Lohe, “Isothermal and thermal-mechanical fatigue of alumina,” *Materialwissenschaft und Werkstofftechnik*, vol. 36, no. 3-4, pp. 136–139, 2005.

- [42] R. V. Marrey, R. Burgermeister, R. B. Grishaber, and R.O. Ritchie, "Fatigue and life prediction for cobalt-chromium stents: a fracture mechanics analysis," *Biomaterials*, vol. 27, no. 9, pp. 1988–2000, 2006.
- [43] F. Guiu, M. J. Reece, and D. A. J. Vaughan, "Cyclic fatigue of ceramics," *Journal of Materials Science*, vol. 26, no. 12, pp. 3275–3286, 1991.
- [44] T. Soma, M. Masuda, M. Matsui, and I. Oda, "Cyclic fatigue testing of ceramic materials," *International Journal of High Technology Ceramics*, vol. 4, no. 2–4, pp. 289–299, 1988.
- [45] K. Wang, J. Geng, D. Jones, and W. Xu, "Comparison of the fracture resistance of dental implants with different abutment taper angles," *Materials Science and Engineering C*, vol. 63, pp. 164–171, 2016.
- [46] M. Niinomi and M. Nakai, "Titanium-based biomaterials for preventing stress shielding between implant devices and bone," *International Journal of Biomaterials*, vol. 2011, Article ID 836587, 10 pages, 2011.
- [47] W. Y. Chang, T. H. Fang, Z. W. Chiu, Y. J. Hsiao, and L. W. Ji, "Nanomechanical properties of array TiO<sub>2</sub> nanotubes," *Microporous and Mesoporous Materials*, vol. 145, no. 1–3, pp. 87–92, 2011.
- [48] G. A. Crawford, N. Chawla, K. Das, S. Bose, and A. Bandyopadhyay, "Microstructure and deformation behaviour of biocompatible TiO<sub>2</sub> nanotubes on titanium substrate," *Acta Biomaterialia*, vol. 3, no. 3, pp. 359–367, 2007.
- [49] FoodandDrugAdministration,2004<http://www.fda.gov/RegulatoryInformation/Guidance/s/ucm072424.htm#4>.